T2R2 東京科学大学 リサーチリポジトリ
Science Tokyo Research Repository

論文 / 著書情報
Article / Book Information

Title	Effects of GeI2 or ZnI2 addition to perovskite CH3NH3PbI3 photovoltaic devices
Authors	Hiroki Tanaka, Yuya Ohishi, Takeo Oku
Citation	AIP Conference Proceedings, Vol. 1929, 1, pp. 020007-1-020007-7
Pub. date	2018, 1
Note	This article may be downloaded for personal use only. Any other use requires prior permission of the author and AIP Publishing. This article appeared in AIP Conference Proceedings, Vol. 1929, 1, pp. 020007-1-020007-7 and may be found at http://dx.doi.org/10.1063/1.5021920.

Powered by T2R2 (Science Tokyo Research Repository)

Effects of GeI_2 or ZnI_2 addition to perovskite $CH_3NH_3PbI_3$ photovoltaic devices

Hiroki Tanaka, Yuya Ohishi, and Takeo Oku

Citation: AIP Conference Proceedings **1929**, 020007 (2018); doi: 10.1063/1.5021920
View online: https://doi.org/10.1063/1.5021920
View Table of Contents: http://aip.scitation.org/toc/apc/1929/1
Published by the American Institute of Physics

Articles you may be interested in

Rietveld refinement of the crystal structure of perovskite solar cells using $CH_3NH_3PbI_3$ and other compounds
AIP Conference Proceedings **1929**, 020003 (2018); 10.1063/1.5021916

Effects of hot airflow during spin-coating process on $CH_3NH_3PbI_{3-x}Cl_x$ perovskite solar cells
AIP Conference Proceedings **1929**, 020005 (2018); 10.1063/1.5021918

Effects of CuBr addition to $CH_3NH_3PbI_3$(Cl) perovskite photovoltaic devices
AIP Conference Proceedings **1929**, 020010 (2018); 10.1063/1.5021923

Fabrication and characterization of rubidium/formamidinium-incorporated methylammonium-lead-halide perovskite solar cells
AIP Conference Proceedings **1929**, 020015 (2018); 10.1063/1.5021928

Fabrication and characterization of perovskite solar cells added with $MnCl_2$, YCl_3 or poly(methyl methacrylate)
AIP Conference Proceedings **1929**, 020012 (2018); 10.1063/1.5021925

Effects of CsBr addition on the performance of $CH_3NH_3PbI_{3-x}Cl_x$-based solar cells
AIP Conference Proceedings **1929**, 020026 (2018); 10.1063/1.5021939

Effects of GeI_2 or ZnI_2 addition to perovskite $CH_3NH_3PbI_3$ photovoltaic devices

Hiroki Tanaka, Yuya Ohishi, and Takeo Oku*

Department of Materials Science, The University of Shiga Prefecture
2500 Hassaka, Hikone, Shiga 522-8533, Japan

*Corresponding author: oku@mat.usp.ac.jp

Abstract. $CH_3NH_3PbI_3$ added with GeI_2 or ZnI_2 perovskite photovoltaic devices were fabricated characterized. The surface coverages of the perovskite layers were improved by the addition of GeI_2 or ZnI_2. Formation of PbI_2 observed for the pristine $CH_3NH_3PbI_3$ was suppressed by the GeI_2 or ZnI_2 addition, which resulted in the improvement of the conversion efficiencies of the perovskite photovoltaic devices.

INTRODUCTION

In recent years, $CH_3NH_3PbI_3$-based perovskite solar cells have much attention because of their high conversion efficiencies and easy fabrication process [1-4]. However, poor durability of the solar cells is a problem for practical use. One of the reason of this poor durability would be instability of the $CH_3NH_3PbI_3$ crystals. It has been reported that the structural transition temperature from a tetragonal structure (a low temperature phase) to a cubic structure (a high temperature phase) is 330 K [5]. This transition temperature is close to room temperature, which resulted in the structural instability at room temperature. In addition, the lead (Pb) is a toxic element, and the photovoltaic devices of the perovskite crystals with reduced Pb are needed for the practical use.

In general, perovskite compounds can be expressed as the chemical formula of ABX_3, where A is a monovalent cation, B is a divalent cation, and X is a monovalent anion. Structural stabilities of the perovskite structure can be estimated by the tolerance factor (t-factor), as shown in Eq. (1) [6-8].

$$t = \frac{R_A + R_X}{\sqrt{2}(R_B + R_X)} \tag{1}$$

The R_A, R_B, and R_X are the ionic radii of the A, B, and X ions, respectively. In the case of the $CH_3NH_3PbI_3$, $CH_3NH_3^+$, Pb^{2+} and I^- ions are located at A, B, and X sites, respectively. When the value of "t" is equal to 1, the perovskite crystal has an ideal cubic structure. The structure of the $CH_3NH_3PbI_3$ perovskite crystal would not be so stable, because the t-factor of the $CH_3NH_3PbI_3$ crystal is 0.912, where the ionic radii of $CH_3NH_3^+$, Pb^{2+}, and I^- are 2.17 Å [9], 1.19 Å [10], and 2.20 Å [10], respectively. If the cation with larger ion radius than that of the Pb^{2+} is introduced to B sites, the t-factor increases and perovskite structure would be stabilized. Since the ionic radius of Ge (0.73 Å) [10] is smaller than those of other group 14 elements such as Pb (1.19 Å) [10] and Sn (1.18 Å) [10], Ge addition to the perovskite crystals would be a suitable method to stabilize the perovskite crystals. The group 12 elements, such as Zn, Cd and Hg, would be the other candidates of additives to the perovskite crystals, because these elements become divalent cations. Among them, ionic radius of Zn (0.73 Å) [10] is smaller than those of Cd (1.19 Å) [10] and Hg (0.95 Å) [10], and Zn could be selected as the additives to the perovskite crystals. Both Cd and Hg are toxic elements, and Zn is nontoxic, therefore, Zn would be a better candidate of additives in group 12 elements.

The Irago Conference 2017
AIP Conf. Proc. 1929, 020007-1–020007-7; https://doi.org/10.1063/1.5021920
Published by AIP Publishing. 978-0-7354-1621-5/$30.00

The purpose of the present work is to fabricate and characterize the $CH_3NH_3PbI_3$ photovoltaic devices added with GeI_2 or ZnI_2. The Ge and Zn elements are expected to stabilize the perovskite structures.

EXPERIMENTAL PROCEDURES

A schematic illustration of the fabricated photovoltaic cells is shown in Fig. 1. The detailed fabrication process was described in the previous reports [11-16]. All process was carried out under ordinary air. F-doped tin oxide (FTO) substrates were cleaned using an ultrasonic bath with acetone and ethanol, and dried under nitrogen gas. Then, FTO substrates were treated with ultra-violet-ozone cleaner (Asumi Giken, ASM401N) for 15 min. TiO_x precursor solutions of 0.15 M and 0.30 M were prepared from titanium diisopropoxide bis (acetyl acetonate) (Sigma Aldrich) with 1-butanol (Wako Pure Chemical Industries). The 0.15 M TiO_x precursor solution was spin-coated on the FTO substrates at 3000 rpm for 30 s using a spin coater (Mikasa, MS-A100) and annealed at 125 °C for 5 min. Then, the 0.30 M TiO_x precursor solution was spin-coated on the TiO_x layer at 3000 rpm for 30 s and annealed at 125 °C for 5 min. The 0.30 M precursor process was performed twice. After that, the FTO substrate was sintered at 500 °C for 30 min to form a compact TiO_2 layer. Mesoporous TiO_2 layer was spin-coated at 5000 rpm for 30 s on the compact TiO_2 layer using TiO_2 paste, which is prepared with TiO_2 powder (Aerosil, P-25) with poly (ethylene glycol) (Nacalai tesque, PEG #20000) in distilled water [17]. This solution was mixed with acetylacetone (Wako Pure Chemical Industries) and triton X-100 surfactant (Sigma Aldrich) for 30 min, and was left to suppress the bubble in the solution for 12 h. The cells were annealed at 120 °C for 5 min and at 500 °C for 30 min to form the mesoporous TiO_2 layer [18].

For the preparation of the perovskite compounds, solutions of CH_3NH_3I (Tokyo Chemical Industry), PbI_2 (Tokyo Chemical Industry) with ZnI_2 (Sigma Aldrich) or GeI_2 (Sigma Aldrich) with γ-butyrolactone (Wako Pure Chemical Industries, 0.3 ml) and *N*,*N*-dimethylformamide (DMF, Sigma-Aldrich, 0.2 ml)) as solvent were mixed at 60 °C. In the case of the standard $CH_3NH_3PbI_3$ precursor, molar concentrations of CH_3NH_3I and PbI_2 were both 1.2 M. The molar concentrations of CH_3NH_3I, PbI_2, and ZnI_2 for the $CH_3NH_3PbI_3$ with ZnI_2 were 1.2 M, 1.08 M and 0.12 M, respectively. On the other hand, since it was difficult to dissolve the GeI_2 in the present solvent, a diluted GeI_2 solution was prepared. The molar concentrations of CH_3NH_3I, PbI_2, and GeI_2 for the $CH_3NH_3PbI_3$ with GeI_2, were 0.6 M, 0.51 M and 0.09 M, respectively. The perovskite precursor solutions were spin-coated 4 times on the mesoporous TiO_2 at 2000 rpm for 60 s. Then, the standard cell and the cell with ZnI_2 were annealed at 100 ℃ for 15 min, and the cell with GeI_2 was annealed at 120 ℃ for 20 min. Next, a hole transport layer (HTL) was prepared by spin-coating. As a HTL, a solution of 2,2',7,7'-tetrakis-[*N*,*N*-di(p-methoxyphenyl)amino]-9'9'-spirobifluorene (spiro-OMeTAD, Sigma Aldrich, 36.1 mg) in chlorobenzene (Wako Pure Chemical Industries, 0.5 mL) was mixed with a solution of lithium bis (trifluoromethylsulfonyl) imide (Tokyo Chemical Industry, 260 mg) in acetonitrile (Nacalai tesque, 0.5 mL) for 24 h. The former solution with 4-tert-butylpyridine (Sigma Aldrich, 14.4 μL) was mixed with the Li-TFSI solution (8.8 μL) for 30 min at 70 °C, and cooled to room temperature. Finally, gold (Au) electrodes were evaporated as top electrodes.

The *J*–*V* characteristics of the photovoltaic cells were measured (Keysight, B2901A) under illumination at 100 mW cm^{-2} by using an AM 1.5 solar simulator (San-ei Electric XES-301S). The solar cells were illuminated through the side of the FTO substrates, and the measurement area was 0.090 cm^2. The microstructures of the perovskite layers were measured by an X-ray diffractometer (Bruker, D2 PHASER), an optical microscope (Nikon, Eclipse E600), and a scanning electron microscope equipped with an EDX detector (Jeol, JSM-6010PLUS/LA).

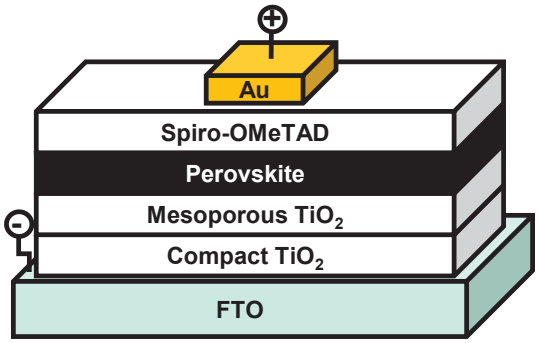

FIGURE 1. Schematic illustration of the present perovskite photovoltaic cell.

RESULTS AND DISCUSSION

The *J-V* characteristics in the forward sweep of the present photovoltaic devices are shown in Fig. 2, which indicates the effects of GeI_2 or ZnI_2 addition to $CH_3NH_3PbI_3$. The measured photovoltaic parameters of the present cells are summarized in Table 1, where V_{OC} is an open-circuit voltage, J_{SC} is a short-circuit current density, *FF* is a fill factor, and η is a conversion efficiency. The standard cell provided a conversion efficiency of 3.54 %, and the cells with GeI_2 or ZnI_2 provided the efficiencies of 6.88, and 5.62 %, respectively. Both GeI_2 and ZnI_2 are effective to improve the conversion efficiencies. The perovskite layer with GeI_2 was supposed to be thin, because of the diluted precursor solution, which resulted in the decrease of J_{SC} value. In spite of the lowest J_{SC} value, the conversion efficiency of the cell with GeI_2 provided the best η value among these three devices, which is due to the highest V_{OC} and *FF*.

XRD patterns of the present cells are shown in Fig. 3. Although most of XRD peaks can be indexed with $CH_3NH_3PbI_3$ for the standard perovskite cell, a strong peak of PbI_2 was observed. The PbI_2 peaks were reduced by adding GeI_2 or ZnI_2 to the $CH_3NH_3PbI_3$, which provided the improvement of the V_{OC} and the conversion efficiencies.

Optical microscope images of the present photovoltaic devices are shown in Fig. 4. Grain sizes of the perovskite decreased by adding the GeI_2. On the other hand, crystal growth was observed by adding ZnI_2. In both cases, the surface coverages of the perovskite layers with GeI_2 or ZnI_2 were higher than that of the standard perovskite cell, which resulted in improvement of V_{OC} and η values.

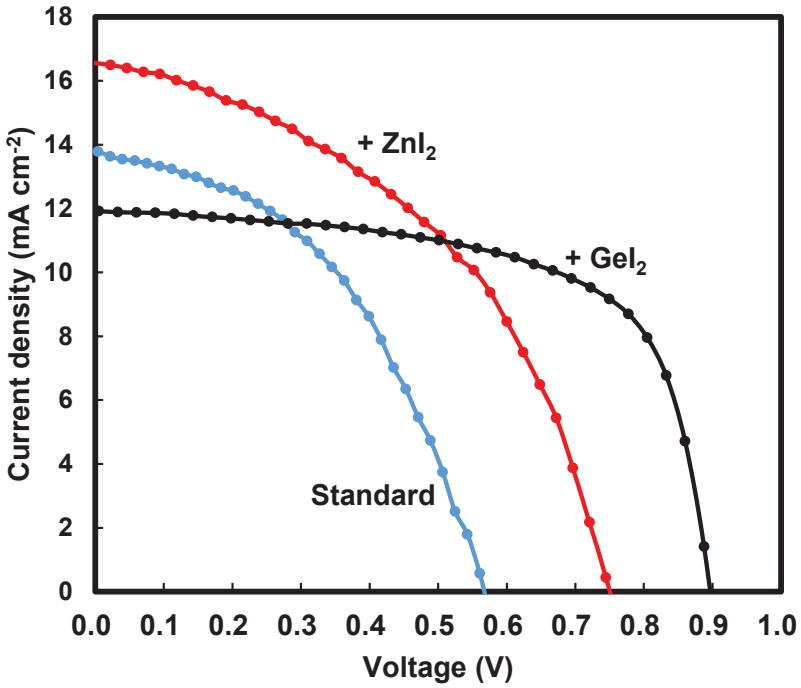

FIGURE 2. *J-V* characteristic of the present perovskite photovoltaic cells.

TABLE 1. Measured parameters of the present perovskite photovoltaic cells.

Devices	J_{SC} (mA cm^{-2})	V_{OC} (V)	*FF*	η (%)
Standard	13.8	0.567	0.452	3.54
+GeI_2	11.9	0.896	0.645	6.88
+ZnI_2	16.6	0.750	0.453	5.62

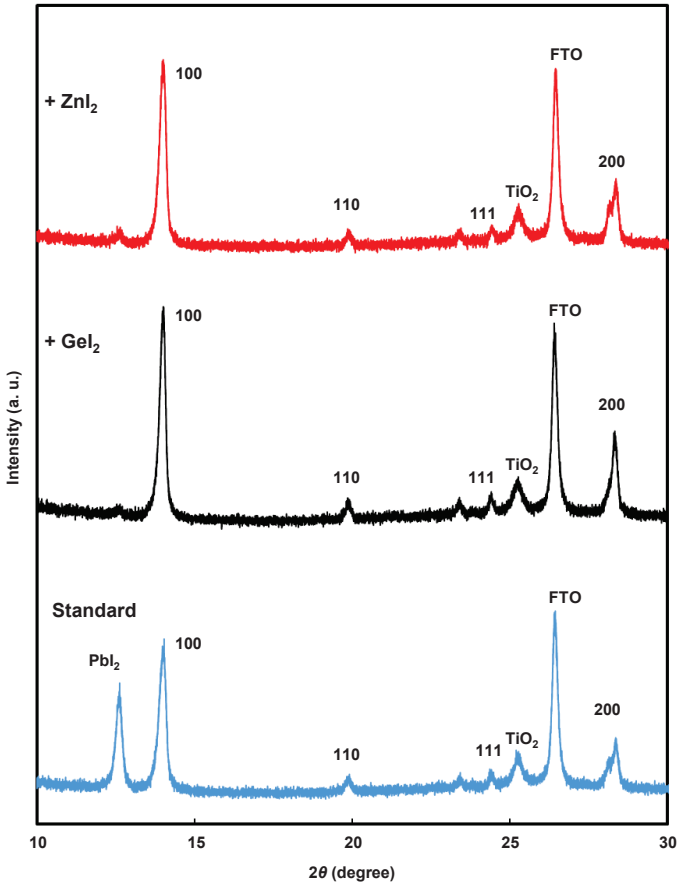

FIGURE 3. XRD patterns of the present perovskite solar cells.

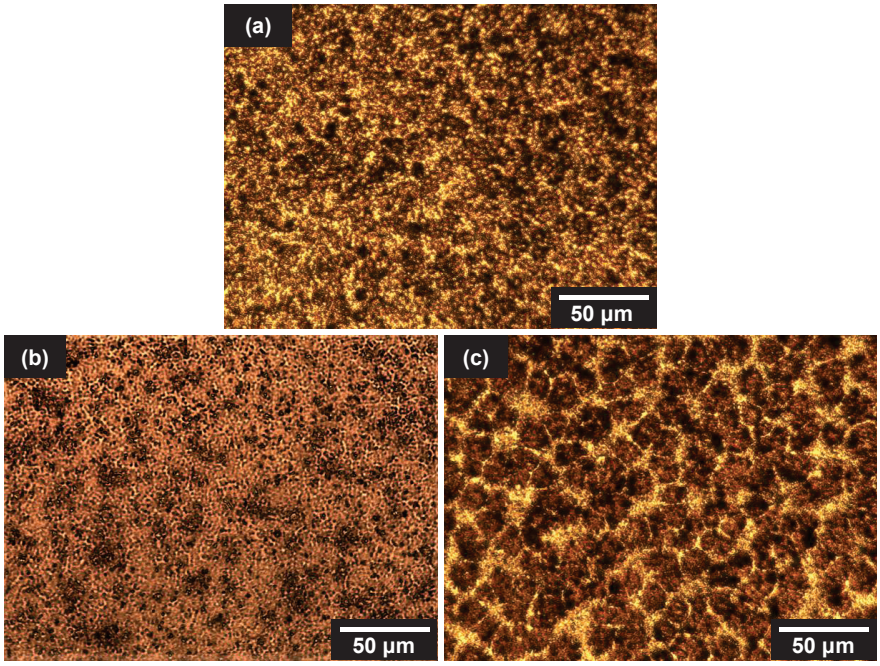

FIGURE 4. Optical microscope images of (a) standard $CH_3NH_3PbI_3$ cell, (b) cell with GeI_2, and (c) cell with ZnI_2

A SEM image of the standard $CH_3NH_3PbI_3$ perovskite cell is shown in Fig. 5(a), and the elemental mapping images of I and Pb are shown in Figs. 5(b) and 5(c), respectively. A SEM image of the $CH_3NH_3PbI_3$ cell with GeI_2 is shown in Fig. 6(a), and the elemental mapping images of I, Pb and Ge are shown in Figs. 6(b)-6(d), respectively. Figure 7 (a) is a SEM image of the perovskite cell with ZnI_2, and the elemental mapping images of I, Pb and Zn are shown in Figs. 7(b)-7(d), respectively. It can be seen that all elements were distributed uniformly in the perovskite crystals. Especially, Ge are distributed in the perovskite layer uniformly, in spite of less solubility of GeI_2 in solvent, which is resulted in the highest V_{OC} and η values among these samples.

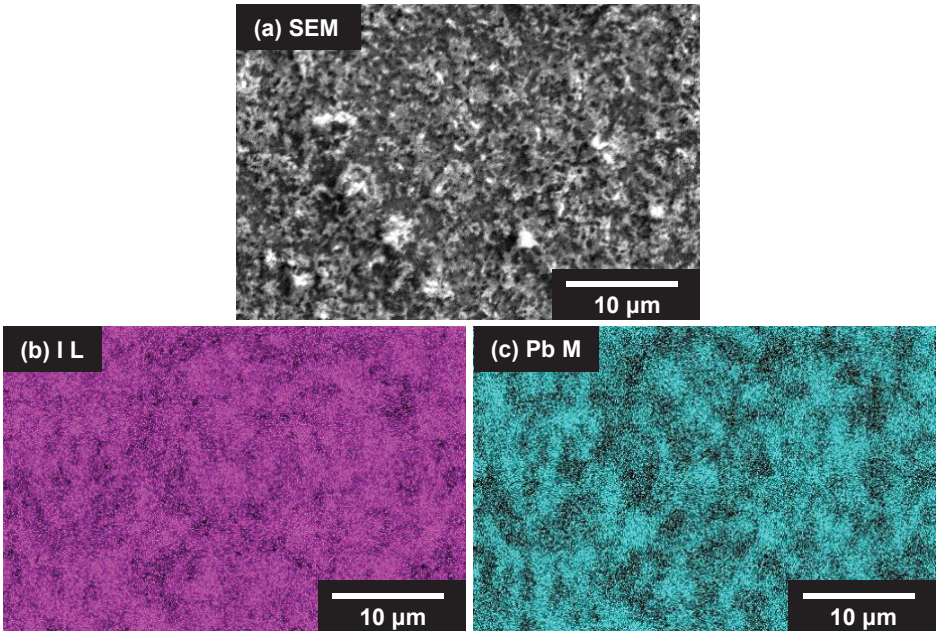

FIGURE 5. (a) SEM image of standard $CH_3NH_3PbI_3$ cell. Elemental mapping images of (b) I L line and (c) Pb M line.

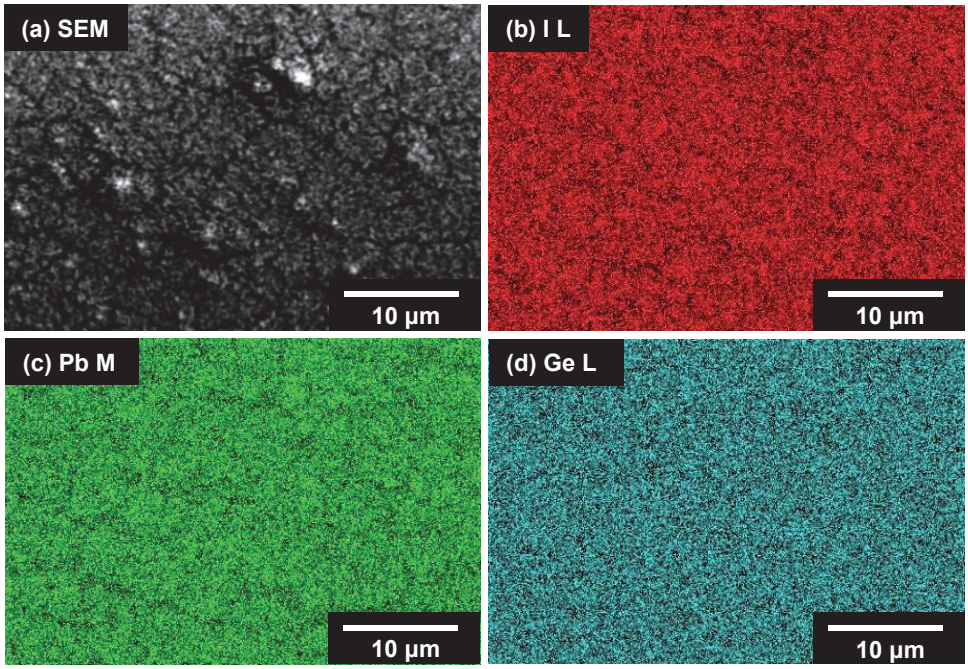

FIGURE 6. (a) SEM image of $CH_3NH_3PbI_3$ cell with GeI_2. Elemental mapping images of (b) I L line, (c) Pb M line, and (d) Ge L line.

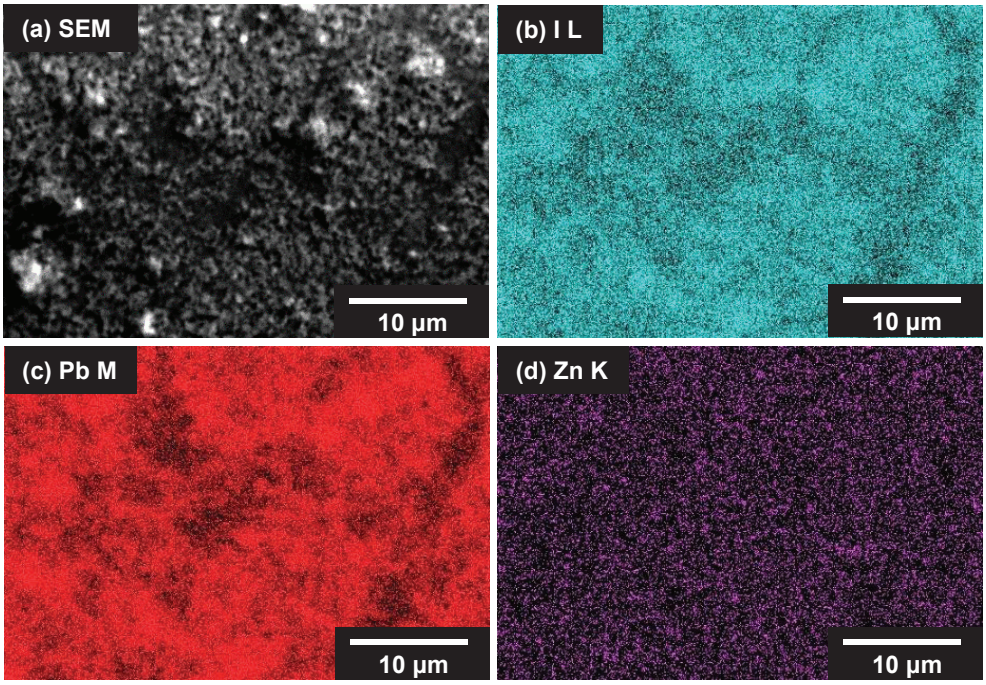

FIGURE 7. (a) SEM image of $CH_3NH_3PbI_3$ cell with ZnI_2. Elemental mapping images of (b) I L line, (c) Pb M line, and (d) Zn K line.

CONCLUSIONS

Effects of GeI_2 or ZnI_2 addition to perovskite $CH_3NH_3PbI_{3-x}Cl_x$ precursor solutions on microstructures and photovoltaic properties were investigated. The perovskite precursor solutions were prepared by dissolving GeI_2, ZnI_2, CH_3NH_3I and PbI_2 to the mixture solvents of γ-butyrolactone and DMF. The present perovskite photovoltaic devices were fabricated by a spin-coating technique in ordinary air. Microstructural analysis indicated that the PbI_2 formation was suppressed by the GeI_2 or ZnI_2 addition, and the surface coverages of $CH_3NH_3PbI_3$ layer were improved by the GeI_2 or ZnI_2 the addition, which resulted in the improvement of photovoltaic properties.

ACKNOWLEDGMENTS

This work was partly supported by Satellite Cluster Program of the Japan Science and Technology Agency.

REFERENCES

1. A. Kojima, K. Teshima, Y. Shirai, and T. Miyasaka, J. Am. Chem. Soc. **131**, 6050–6051 (2009).
2. J.H. Im, C.R. Lee, J.W. Lee, S.W. Park, and N.G. Park, Nanoscale **3**, 4088-4093 (2011).
3. H.S. Kim, C.R. Lee, J.H. Im, K.B. Lee, T. Moehl, A. Marchioro, S.J. Moon, R. Humphry-Baker, J.H. Yum, J.E. Moser, M. Grätzel, and N. G. Park, Sci. Rep. **2**, 591 (2012).
4. I. Grinberg, D. V. West, M. Torres, G. Gou, D. M. Stein, L. Wu, G. Chen, E. M. Gallo, A. R. Akbashev, P. K. Davies, J. E. Spanier and A. M. Rappe, Nature **503**, 509-512 (2013).
5. T. Oku, *Solar Cells and Energy Materials* (Walter de Gruyter, Berlin, 2017), pp. 109-151.
6. V. M. Goldschmidt, Die Naturwissenschaften. **21,** 477-485 (1926).
7. S.F. Hoefler, G. Trimmel, and T. Rath, Monatsh. Chem. **148**, 795-826 (2017).
8. M. A. Green, A. Ho-Baillie, and H. J. Snaith, Nat. Photonics **8**, 506-514 (2014).
9. G. Kieslich, S. Sun, and A.K. Cheetham, Chem. Sci. **5**, 4712-4715 (2014).
10. J.A. Dean, *Lange's Handbook of Chemistry* (McGRAW-HILL, New York, 1999) 15th ed., sect. 4.

11. N. Ueoka, N., Y. Ohishi, Y. Shirahata, A. Suzuki, T. Oku, AIP Conf. Proc. **1709**, 020020-1-020020-9 (2016).
12. T. Oku, Y. Ohishi, A. Suzuki, and Y. Miyazawa, Metals **6**, 147 (2016).
13. M. Zushi, A. Suzuki, T. Akiyama, and T. Oku, Chem. Lett. **43**, 916 (2014).
14. T. Oku, M. Zushi, Y. Imanishi, A. Suzuki, and K. Suzuki, Appl. Phys. Express **7**, 121601-1-121601-4 (2014).
15. T. Oku, Y. Ohishi, and A. Suzuki, Chem. Lett. **45**, 134-136 (2016).
16. T. Hamatani, Y. Shirahata, Y. Ohishi, M. Fukaya, and T.Oku, Adv. Mater. Phys. Chem. **7**, 1-10 (2017).
17. T. Oku, N. Kakuta, K. Kobayashi, A. Suzuki, and K. Kikuchi, Prog. Nat. Sci. Mater. Int., 21, 122-126 (2011).
18. T. Oku, K. Suzuki, and A. Suzuki, J. Ceram. Soc. Jpn. **124**, 234-238 (2016).